

An Intrinsic Smoothing Mechanism For Gamma-Ray Burst Spectra in the Fireball Model

Renyue Cen

Princeton University Observatory, Princeton University, Princeton, NJ 08544

cen@astro.princeton.edu

Received _____; accepted _____

arXiv:astro-ph/9904125v4 22 Aug 1999

ABSTRACT

It is shown that differential Doppler shift of different patches of the blastwave front in the fireball model at varying angles to the line of sight could provide an intrinsic smoothing mechanism for the spectra of gamma-ray bursts (GRBs) and the associated afterglows at lower energy bands. For the model parameters of interest, it is illustrated that a monochromatic spectrum at ν in blastwave comoving frame is smoothed and observed to have a half-width-half-maximum (HWHM) of $\sim (0.6 - 2.0)\nu$. Some other implications of this smoothing process are discussed. In particular, if the circumburster medium is uniform and electron and magnetic energies are fixed fractions of the total post-shock energy with time, the observed GRB or afterglow spectra cannot be steeper than $\nu^{-\alpha}$ with $\alpha = 0.75 - 1.25$, regardless of the intrinsic spectra in the comoving shock frame; i.e., a very steep electron distribution function (with $p > 3$) could produced an observed spectrum with $\alpha \sim 1$. In addition, a generic fast-rise-slow-decay type of GRB temporal profile is expected.

Subject headings: gamma rays: bursts – hydrodynamics – relativity – shock waves

1. Introduction

It is remarkable that the simple fireball model for cosmological gamma-ray bursts can explain the many major features of the gamma-ray bursts and their afterglows (Rees & Mészáros 1992, 1994; Paczynski & Rhodes 1993; Wijers, Rees, & Mészáros 1997; Vietri 1997a,b; Waxman 1997a,b; Reichart 1997; Katz & Piran 1997; Sari 1997). It is noted, however, that the fireball model may produce multiple spectral components due to the existence of both the forward and reverse shocks at least at some time period (e.g., Mészáros, Rees, & Papathanassiou 1994). Moreover, reprocessing of the primary spectrum by, for example, inverse Compton scattering (e.g., Pilla & Loeb 1998), introduces additional features to the spectra, even if it is initially featureless. Finally, resonant line features or recombination lines due to heavy elements, for example, in dense blobs as discussed in Mészáros & Rees (1998), may add additional features to the continuum. In this *Letter* it is pointed out that spectral smoothing due to differentially varying Doppler shift for different patches of the fireball at varying angles to the line of sight provides an intrinsic, unavoidable smoothing mechanism. While this effect is fairly well known, a more quantitative analysis focusing on the case of GRBs is useful. This *Letter* presents such a semi-quantitative analysis.

2. Differential Doppler Shift Across a Fireball Front

For the present illustration I assume that the GRB fireball is spherical and homogeneous, for which a single parameter, θ , the angle to the burster-observer vector, is sufficient to characterize the direction of a traveling patch of shock heated, radiation emitting material. It is convenient to use the time measured in the rest-frame of the burster, t , as the independent variable to express other quantities.

First, one has to find the relation between time t for a fireball patch at θ and the time measured by the observer on the Earth (called “ O ” hereafter), t_{obs} , i.e., the arrival time.

Since the *apparent* perpendicular traveling speed of a patch with θ seen by O is

$$\beta_{\perp}(t) = \frac{\beta(t) \sin \theta}{1 - \beta(t) \cos \theta} \quad (1)$$

in units of the speed of light, where $\beta(t)$ is the spherical expansion speed of the fireball in the rest-frame of the burster. By definition, $\beta_{\perp}(t)$ is

$$\beta_{\perp}(t) = \frac{dr}{dt_{obs}} \sin \theta. \quad (2)$$

Combining equations (1, 2) gives

$$\frac{dr}{dt_{obs}} = \frac{\beta(t)}{1 - \beta(t) \cos \theta}. \quad (3)$$

Since one also has the following relation

$$\frac{dr}{dt} = \beta(t), \quad (4)$$

one finds the equation relating t_{obs} to t :

$$\frac{dt_{obs}}{dt} = 1 - \beta(t) \cos \theta. \quad (5)$$

Next, to have a tractable treatment, it is assumed that the Lorentz factor, $\Gamma(t) \equiv 1/\sqrt{1 - \beta(t)^2}$, has the following simplified evolution: it is constant (equal to Γ_i) at $t \leq t_{dec}$ and decays at $t > t_{dec}$ as

$$\Gamma = \Gamma_i \left(\frac{t}{t_{dec}} \right)^{-\alpha}, \quad (6)$$

where Γ_i is the initial Lorentz factor and t_{dec} (measured in the rest-frame of the burster) characterizes the transition time after which deceleration of the fireball expansion becomes significant (hence the fireball kinetic energy can be converted into radiation) and can be expressed approximately as $t_{dec} = \left(\frac{3E}{4\pi\Gamma_i^2 c^5 m_p n} \right)^{1/3}$ (Blandford & McKee 1976), where E is

the initial fireball energy, n is the density of the circumburst medium (which is assumed to be uniform, for simplicity) and other notations are conventional. Note that $\alpha = 3$, if the fireball cools radiatively efficiently, and $\alpha = 3/2$, if the fireball cools only adiabatically.

To make the point in a simple way it is assumed that the total luminosity per unit frequency (in the comoving frame) of the shock front at a fixed time t is a delta function in frequency (i.e., a monochromatic spectrum):

$$L_\nu(\nu', t) = C(t)\delta[\nu' - \nu_0(t)] \quad (7)$$

in the frame comoving with the blastwave. The characteristic frequency $\nu_0(t)$ at time t in the comoving frame is parameterized as

$$\nu_0(t) = A\left(\frac{\Gamma}{\Gamma_i}\right)^\psi, \quad (8)$$

where A is a constant. Note that, in the case of synchrotron radiation and assuming that both the electron thermal energy density and the magnetic energy density are fixed fractions of the post-shock nucleon thermal energy density, one has $\psi = 3$. $C(t)$ is expressed as

$$C(t) = B\left(\frac{t}{t_{dec}}\right)^\xi, \quad (9)$$

where B is another constant and the ξ parameterizes the temporal profile of the amplitude of the radiation.

At a given time O receives radiation from *different parts across the fireball surface*, emitted at varying times in the burster frame; i.e., radiation from regions of varying θ at varying t [see equation (5) for the relation between t and t_{obs}] is seen by O at the same time (Sari 1998). The received frequency of the radiation at t_{obs} from region with θ emitted at t is

$$\nu(t_{obs}) = \nu_0(t)D(\theta, t), \quad (10)$$

where $D(\theta, t)$ is the Doppler factor for regions with θ at time t :

$$D(\theta, t) = \frac{1}{\Gamma(t)[1 - \beta(t) \cos \theta]}. \quad (11)$$

The flux density observed by O at frequency ν at time t_{obs} is

$$S(\nu, t_{obs}) = \frac{1}{8\pi d^2} \int_{-1}^1 L_\nu(\nu', t) D^3(\theta, t) d\mu \quad (12)$$

where $\nu' (= \nu/D)$ is the frequency in the blastwave frame, d is the distance of the GRB from O and $\mu \equiv \cos \theta$. Combining equations (10,11) gives

$$d\mu = \left(\frac{1 - \beta\mu}{\beta} \right) \frac{d\nu}{\nu}. \quad (13)$$

Inserting equations (7,13) into equation (12) and integrating over ν give

$$S(\nu, t_{obs}) = \frac{C(t)}{8\pi d^2 \nu_0(t)} D^3(\theta, t) \frac{1 - \beta(t) \cos \theta}{\beta(t)}. \quad (14)$$

Note that $S(\nu, t_{obs})$ is in a parametric form; given t_{obs} , one can determine the burster frame time t for a given patch at θ using equation (5). Then, one determines $S(\nu, t_{obs})$ using equation (14) combined with equations (6,8,9,11), given t and θ . Meantime, $\nu(t_{obs})$ is related to t and θ by equation (10). Thus, one can find $S(\nu, t_{obs})$ as a function of $\nu(t_{obs})$ at t_{obs} . Let us consider a few simple but relevant cases to illustrate the effect.

Case 1: $\alpha = 3/2$, $\psi = 0$ and $\xi = 0$. This case may have some bearing on such radiation features as atomic line features whose intrinsic frequencies are independent of t (i.e., $\psi = 0$).

Case 2: $\alpha = 3$, $\psi = 3$ and $\xi = 1$. This case may be related to the epoch where radiative cooling is efficient and intensity at the frequency in question is still rising, which could be relevant for radiation at frequencies lower than the peak of the synchrotron radiation spectrum (due to a truncated power-law electron distribution) at early times of a GRB event.

Case 3: $\alpha = 3$, $\psi = 3$ and $\xi = -1$. This may be related to the epoch where radiative cooling is efficient and intensity at the frequency in question has started to decrease, which could

be relevant for radiation at frequencies higher than the peak frequency of the spectrum at early times of a GRB event.

Case 4: $\alpha = 3/2$, $\psi = 3$ and $\xi = 1$, This case is similar to Case (2) with the primary difference that radiative cooling is unimportant here. This may be relevant for GRB afterglows such as the radio afterglows when electron cooling time is likely to be significantly longer than the dynamic time of the expanding fireball at frequencies lower than the peak frequency of the spectrum.

Case 5: $\alpha = 3/2$, $\psi = 3$ and $\xi = -1$, This case is similar to Case 4 but for frequencies higher than the peak frequency of the spectrum.

While it is convenient to express various quantities using t as the independent time variable, one needs to express the final observables using t_{obs} , which is related to t (for $\theta = 0$; see equation 5) as

$$t_{obs} = \frac{t_{dec}}{2\Gamma_i^2} \left[1 + \frac{1}{2\alpha + 1} \left(\frac{t}{t_{dec}} \right)^{2\alpha+1} \right] \quad (15)$$

for the simplified solution of $\Gamma(t)$ given by equation (6). Figure (1a) shows the flux density as a function of frequency at $t_{obs} = t_{dec}/\Gamma_i^2$ for the five cases. The frequency is normalized such that unity corresponds to the radiation from regions with $\theta = 0$ and the flux density is normalized to be unity at unity frequency. The sharp turns to the left for cases (ii,iii,iv,v) correspond to the sharp turn of the evolution of the Lorentz factor at $t = t_{dec}$. Figure (1b) shows the flux density as a function of frequency at $t_{obs} = 5000t_{dec}/\Gamma_i^2$ for the five cases. Also shown in both panels are two straight lines in the upper right corner indicating the spectral slope of -0.75 and 1.25 , respectively, which bracket the range of the spectral slope for various cases shown. Note that sharp turns as seen in (1a) are not visible simply because they appear at much lower intensity level than the displayed range in the figure. Note that $t_{dec} = 16 \left(\frac{E}{10^{52}\text{erg}} \right)^{1/3} \left(\frac{\Gamma_i}{300} \right)^{-2/3} \left(\frac{n}{1\text{cm}^{-3}} \right)^{-1/3}$ days. Therefore, for typical values of E , Γ_i and n , t_{obs} is of order a second and a day, respectively, after the fireball explosion for the

two cases shown in (1a) and (1b). These two cases may respectively be relevant for bursts in gamma-ray and afterglows at lower energy bands. It should be noted that, although the external shock model is used to illustrate the smoothing magnitude, the results should be applicable to the internal shock model as well.

Recall that in all cases a delta function spectrum at ν is assumed in the comoving frame at a given time. One sees that this delta function spectrum is smoothed out to appear as a broad spectrum with a half-width-half-maximum (HWHM) of $\sim (0.6 - 2.0)\nu$ for all the cases considered, except for Case 1 where HWHM is $\sim 0.1\nu$. An immediate implication from Figure 1 (see the dot-long-dashed curves on the upper right corner in the two panels) is that the observed spectra of GRBs or their afterglows should roughly have ν^{-1} , if the electron distribution function power index p is equal to greater than 3. In other words, *the observed spectra cannot be steeper than ν^{-1} regardless the value of p* . This slope \propto

It is of interest to understand where the different radiation that correspond to different frequencies in Figure 1 comes from. Figure 2 shows the frequency seen by O at a given time as a function of the emission shell radius from the burster, r , expressed in units of ct_{dec} . It is seen that, for realistic cases (ii,iii,iv,v) that correspond to the continuum radiation of the GRBs and afterglows, higher frequency radiation comes from earlier time t (in the burster frame) with larger angle θ up to t_{dec} after which there is a downturn to lower frequency at still earlier times due to assumed constancy of Γ thus constancy of $\nu_0(t)$. For case (i) lower frequency radiation comes from earlier time t with larger θ . In both panels (a,b) also shown along the solid curves using solid dots are the corresponding θ values in degrees. Dotted and dashed curves are also punctuated by open circles and open squares, corresponding to the same θ values.

3. Discussion

It is shown that differentially varying Doppler boost of different patches of the fireball front provides an intrinsic, unavoidable smoothing mechanism for the spectra of gamma-ray bursts and their afterglows. The detailed smoothing patterns are complicated, depending upon various factors such as the evolution of the Lorentz factor and the evolution of the intrinsic (i.e., comoving frame) radiation spectrum. Nonetheless, for plausible ranges of model parameters of interest, a comoving frame delta function spectrum at ν is smoothed to have a HWHM of $\sim (0.6 - 2.0)\nu$, assuming that the time evolution of the characteristic frequency $\nu(t)$ is proportional to some positive power of the shock front Lorentz factor, Γ^ψ (where $\psi > 0$; see equation 8). This type of smoothing may be applicable to continuous spectra such as from synchrotron mechanism.

In the case $\psi = 0$ (appropriate for atomic line features which are independent of the blastwave dynamics), the spectral smoothing is smaller, with a HWHM of $\sim 0.1\nu$. Thus, a sharp linelike emission feature (in the comoving frame) would be smoothed out to have an equivalent width of about 0.1ν . Furthermore, the spectral profile of such a feature will be asymmetrical with a sharp cutoff at the high end (see the two solid curves in Figure 1).

Two interesting and natural consequences arise due to the differential Doppler smoothing. First, the observed spectra of GRBs or their afterglows cannot be steeper than $\nu^{-\alpha}$ with $\alpha = 0.75 - 1.25$ (Figure 1), even though the intrinsic spectra in the comoving shock frame may be much steeper, if the circumburster medium is uniform and electron and magnetic energies are fixed fractions of the total post-shock energy with time. Second, a generic fast-rise-slow-decay type temporal profile of the GRB bursts is expected, not necessarily reflecting the intrinsic temporal profiles of the bursts in the comoving frame. This can be easily seen by considering the case where the intrinsic (blastwave frame) spectrum is a bivariate delta function in both time and frequency. In this case the fast rise

occurs when the radiation from the region around $\theta = 0$ enters the observer's finite band. Subsequently, radiation from regions with gradually increasing θ is received at decreasing amplitudes in the same observer's finite band with a decaying time scale of $\sim t_{dec}/2\Gamma^2$ (in observer's frame).

The work is supported in part by grants AST9318185 and ASC9740300. I thank Bohdan Paczyński for discussion.

REFERENCES

- Blandford, R.D., & McKee, C.F. 1976, *Phys. Fluids*, 19, 1130
- Katz, J., & Piran, T. 1997, *ApJ*, 490, 772
- Mészáros, P., & Rees, M.J. 1998, *ApJ*, 502, L105
- Mészáros, P., Rees, M.J., & Papathanassiou, H. 1994, *ApJ*, 432, 181
- Paczynski, B., & Rhodes, J. 1993, *ApJ*, 418, L5
- Pilla, R.P., & Loeb, A. 1998, *ApJ*, 495, 597
- Rees, M.J., & Mészáros, P. 1992, *MNRAS*, 258, 41
- Rees, M.J., & Mészáros, P. 1994, *ApJ*, 430, L93
- Reichart, D.E. 1997, *ApJ*, 485, L57
- Sari, R. 1997, *ApJ*, 489, L37
- Sari, R. 1998, *ApJ*, 494, L49
- Vietri, M. 1997a, *ApJ*, 478, L9
- Vietri, M. 1997b, *ApJ*, 488, L105
- Waxman, E. 1997a, *ApJ*, 485, L5
- Waxman, E. 1997b, *ApJ*, 489, L33
- Wijers, A.M.J., Rees, M., & Mészáros, P. 1997, *MNRAS*, 288, L51

Fig. 1.— Panels (a,b) shows the flux density as a function of frequency for the five cases (see text). at $t_{obs} = t_{dec}/\Gamma_i^2$ and $t_{obs} = 5000t_{dec}/\Gamma_i^2$, respectively. A fiducial value of $\Gamma_i = 300$ is used. In both panels there are two straight lines in the upper right corner showing the spectral slope of -0.75 and 1.25 , respectively, which approximately bracket the range of the spectral slope for various cases shown.

Fig. 2.— shows the frequency seen by O at a given time as a function of the emission shell radius from the burster r , expressed in units of ct_{dec} for the five cases, with panel (a) at $t_{obs} = t_{dec}/\Gamma_i^2$ and panel (b) at $t_{obs} = 5000t_{dec}/\Gamma_i^2$. A fiducial value of $\Gamma_i = 300$ is used. In both panels also shown along the solid curves using solid dots are the corresponding θ values in degrees. Dotted and dashed curves are also punctuated by open circles and open squares, corresponding to the same θ values.

Figure 1

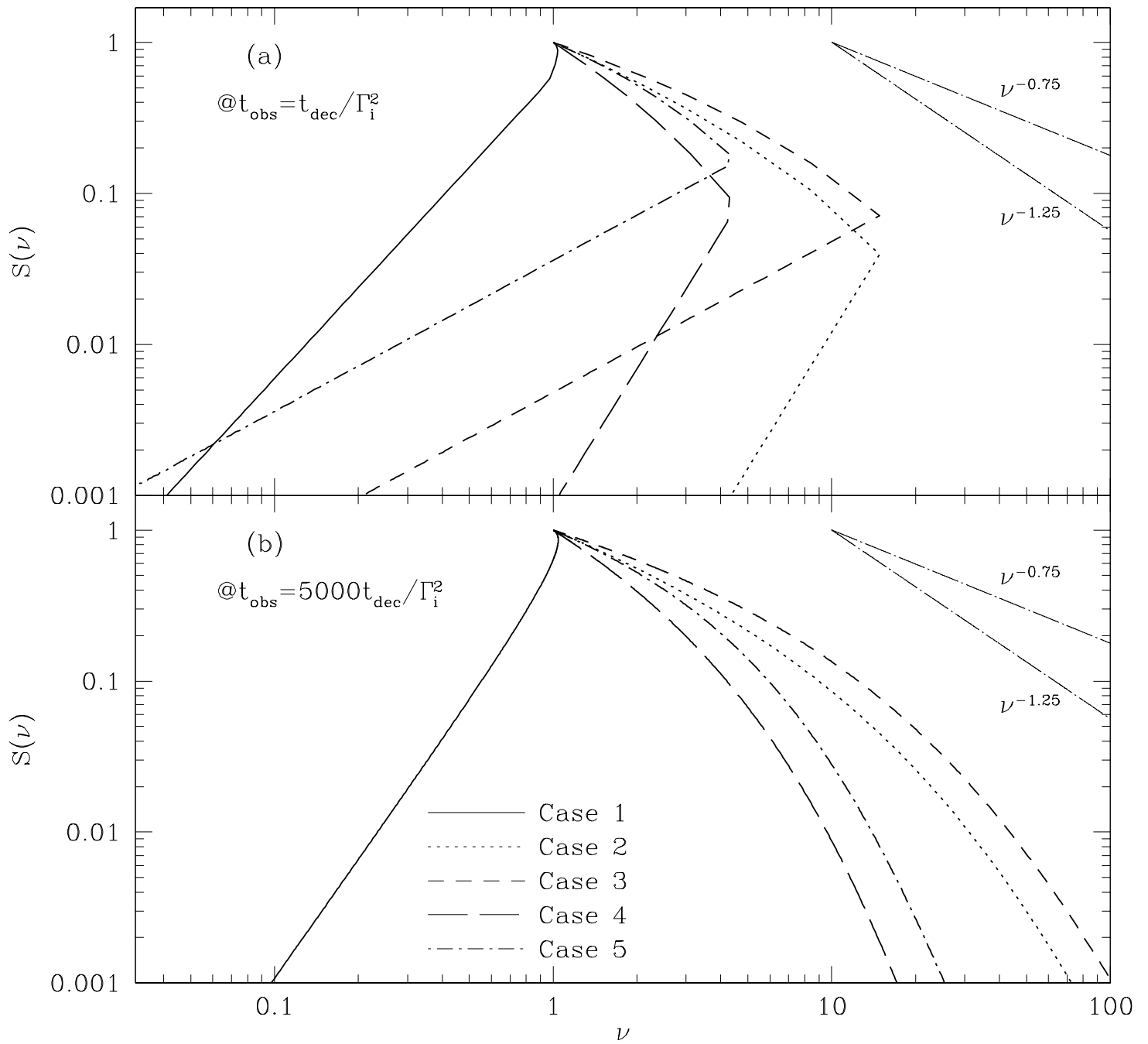


Figure 2

